# Magnetic and electrical properties of Cr- and Ni-doped β - Fe Si 2 single crystals

E. Arushanov, K. Nenkov, D. Eckert, H. Vinzelberg, U. K. Rößler, G. Behr, K.-H. Müller, and J. Schumann

Citation: Journal of Applied Physics **96**, 2115 (2004); doi: 10.1063/1.1768618
View online: http://dx.doi.org/10.1063/1.1768618
View Table of Contents: http://scitation.aip.org/content/aip/journal/jap/96/4?ver=pdfcov
Published by the AIP Publishing





# Magnetic and electrical properties of Cr- and Ni-doped $\beta$-$FeSi_2$ single crystals

E. Arushanov
*Leibniz Institute for Solid State and Materials Research Dresden, P.O. Box 27 01 16, D-01171 Dresden, Germany and Institute of Applied Physics, Academy of Sciences of Moldova, 277028 Chisinau, Moldova*

K. Nenkov, D. Eckert, H. Vinzelberg, U. K. Rößler, G. Behr, K.-H. Müller, and J. Schumann[a)]
*Leibniz Institute for Solid State and Materials Research Dresden, P.O. Box 27 01 16, D-01171 Dresden, Germany*

(Received 22 December 2003; accepted 12 May 2004)

The magnetization, magnetic susceptibility, and resistivity for Cr-doped *p* type and Ni-doped *n* type $FeSi_2$ single crystals have been investigated. The values of the paramagnetic Curie temperature as well as the activation energy of the donor levels are estimated. It is also shown that the magnetization behavior of Cr- and Ni-doped samples significantly depends on the cooling regime: cooling in zero external field and cooling with external field. This resembles the properties of spin glasses and indicates the presence of coupling between magnetic centers. The results of resistivity measurements are analyzed within the framework of different hopping conductivity models. Both the *Mott* and the *Shklovskii-Efros* regime of the variable-range hopping is observed. The values of the characteristic and transition temperatures and the width of the Coulomb quasigap are determined. © *2003 American Institute of Physics*. [DOI: 10.1063/1.1768618]

## I. INTRODUCTION

Silicides form an interesting and important group of compounds compatible with state-of-the-art silicon semiconductor technology. While the majority of the transition metal silicides have a metallic character, some of them, including beta-iron disilicide ($\beta$-$FeSi_2$) show semiconducting properties. $\beta$-$FeSi_2$ has received considerable attention as an attractive material for optoelectronic and thermoelectric applications.[1–3] Recently, observations of electroluminescence at low temperature with a wavelength of 1.5 $\mu$m (Ref. 4) and at room temperature with a wavelength of 1.6 $\mu$m (Ref. 5) have been reported. This has increased the interest in this material and the possibility of its application. Also a solar cell project based on $\beta$-$FeSi_2$ is included in the Japanese program of "Investigation for innovative photovoltaic technology" with a target of up to 8% efficiency.[6]

Transport and optical properties of $\beta$-$FeSi_2$ have been mainly studied so far (see Refs. 1 and 2 and references therein). Reports on magnetic properties are fewer and the results often are not in agreement with each other. At low temperatures a diamagnetic behavior was found on pure $\beta$-$FeSi_2$ polycrystals.[7] A study of polycrystalline $\beta$-$FeSi_2$ films led to the conclusion that $\beta$-$FeSi_2$ behaves as a ferromagnetic material at temperatures below 100 K;[8] however, no evidence of a ferromagnetic phase transition at low temperatures was detected in $\beta$-$FeSi_2$ crystals[9–11] and thin films.[12] Above-mentioned data show that the magnetic properties of $\beta$-iron disilicide are not yet well understood and need to be studied in more detail. It should also be mentioned that some anomalies in the transport properties of $\beta$-$FeSi_2$ were reported, which seem to be related to a magnetic ordering. These are a nonlinear dependence of the Hall resistivity on the magnetic induction[8,9,13] and a hysteresis effect of the Hall resistivity.[14] These findings were explained by the transition of $\beta$-$FeSi_2$ into a magnetic phase at low temperatures[8,14] or by the contribution of light and heavy electrons for the conductivity.[9] Measurements of the time dependence of the remanent Hall voltage for Cr-doped $\beta$-$FeSi_2$ crystals showing a strong hysteresis at low temperatures were performed and a slow time decay of the Hall voltage ascribed to superparamagnetic clusters in the samples was observed at low temperatures.[15]

Electron paramagnetic resonance (EPR) studies applied to $\beta$-$FeSi_2$ single crystals and ceramics reveal a variety of paramagnetic centers.[16–18] Most of the paramagnetic centers observed in single crystals arise from isolated iron group impurities. The 3d transition metals Cr, Mn, and Co, and with less certainty Ni and Cu have been identified.[16]

$\beta$-$FeSi_2$ shows a very narrow range of homogeneity near the atomic ratio Si/Fe of 2.[19] Recently Cr- and Ni-doped $\beta$-$FeSi_2$ single crystals were grown. In most cases the composition of the starting material was equal to the atomic ratio Fe/Si=2 of the disilicide. The Si/Fe atomic ratios of 2.5 and 1.5 in the starting materials for chemical transport growth process were chosen to ensure a crystal formation at the upper and the lower boundaries of the homogeneity range of the $\beta$-$FeSi_2$ phase, too.[20] For $\beta$-$FeSi_2$ used as thermoelectric functional material[20] Cr and Ni were identified as effective acceptor and donor elements, respectively. Transport measurement for Cr- (Ref. 20–23) and Ni-doped[20,24] crystals between 4 and 300 K show an extrinsic behavior with exponential increase of the resistivity with decreasing

[a)]Electronic mail: j.schumann@ifw-dresden.de

 

temperature. The reported values of the activation energy of the Cr acceptor are equal to 85–95 meV,[20–22] 116 meV,[23] and for the Ni donor 95 meV,[20] 150 meV.[24] Presently available experimental data for $\beta$-$FeSi_2$ have been mainly obtained on the basis of electrical measurements. However, the reported anomalies in the transport phenomena seem to be related to magnetic ordering.

Here, we report the results of magnetization and magnetic susceptibility measurements for Cr- and Ni-doped $\beta$-$FeSi_2$ single crystals. The knowledge of the magnetic properties of $\beta$-iron disilicide single crystals can contribute to a better understanding of the nature of the anomalies observed in the transport properties of $\beta$-$FeSi_2$. Data on resistivity measurements are also presented and analyzed within the framework of the *Mott* and the *Shklovskii-Efros* hopping conductivity models.

## II. EXPERIMENT

$\beta$-$FeSi_2$ needlelike single crystals were grown by chemical vapor transport using iodine as a transport agent and with a Si/Fe starting ratio in the transport ampoule of 2.5 allowing a crystal growth at the upper phase boundary of the $\beta$ phase.[19] Cr or Ni (1 at %) was used as dopant. The Si/Fe +(Cr/Ni) ratio in the crystals was near 2 measured by microprobe analysis.

The magnetization ($M$) was measured at various temperatures in the range 5–300 K in magnetic fields $H$ up to 8 kOe using a superconducting quantum interference device magnetometer. The resistivity was studied by standard dc techniques in the same temperature range. For the studied Ni-doped single crystals the magnetization measured at 1 kOe was used to determine the temperature dependence of susceptibility. The mass as well as the values of the magnetization of individual $\beta$-$FeSi_2$ needlelike single crystals are small. Therefore, several single crystals grown under the same technological conditions were measured together as an ensemble with [010] axis parallel to field direction.

## III. RESULTS AND DISCUSSION

### A. Magnetic properties

Our experimental data on the magnetic field dependence of the magnetization ($M$) of Cr- and Ni-doped $\beta$-$FeSi_2$ single crystals are presented in Figs. 1(a) and 1(b), respectively. The values of $M$ are positive and quite small for all crystals studied. The magnetization at the temperature range studied show for the Ni-doped sample a linear behavior with increasing magnetic field up to about 1–2 kOe, a deviation from linearity and a tendency to saturation at higher magnetic fields. For Cr-doped samples a nonlinear magnetic field dependence and a minimum of the values of $M$ in dependence on temperature (at 80–160 K) is observed. Small but nonzero remanent values of magnetization $M_0$ were observed in the measurements on the doped samples. $M_0$ is equal to about $10^{-5}$ and $10^{-3}$ emu/g at low temperature for Cr- and Ni-doped samples, respectively.

The temperature dependencies of the magnetic susceptibility $\chi(T)$ in $n$-type Ni-doped $\beta$-$FeSi_2$ single crystals show a

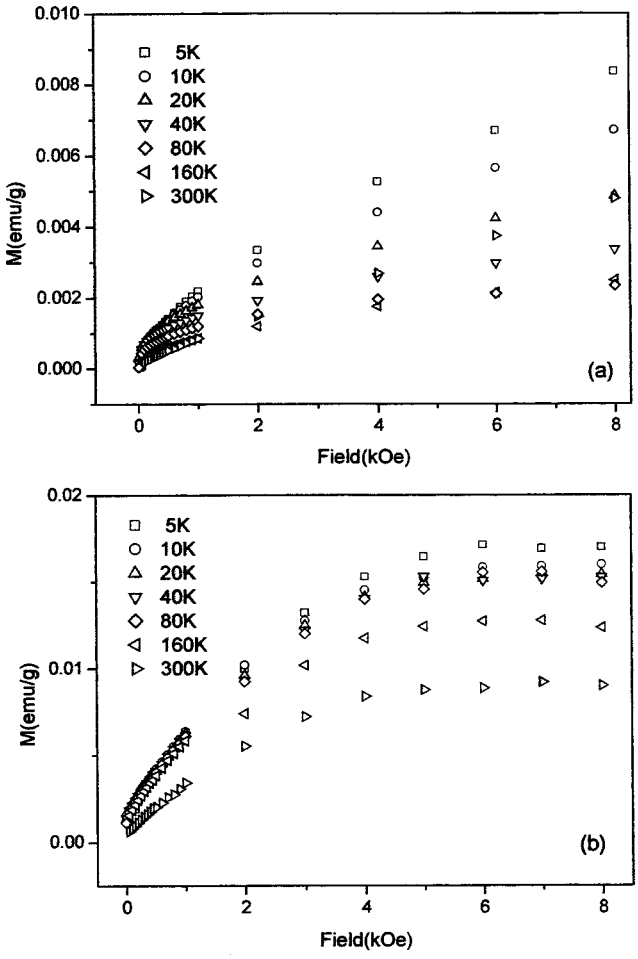


FIG. 1. Magnetization vs magnetic field for Cr-doped (a) and Ni-doped (b) $\beta$-$FeSi_2$ single crystals measured at different temperatures.

decrease of the magnetic susceptibility with increasing temperature (Fig. 2). A fit of our experimental curve $\chi(T)$ has been made using[10]

$$\chi(T) = \chi_o + \chi_p(T) + \chi_c(T), \tag{1}$$

where $\chi_0$ contains a temperature-independent contribution from the lattice, lattice defects, and/or any neutral impurities,

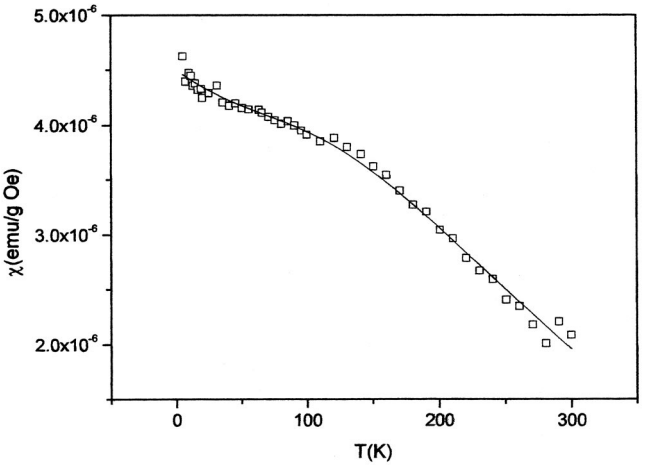


FIG. 2. Magnetic susceptibility vs temperature for the Ni-doped samples [open symbols are the experimental points, the solid curve corresponds to a fit based on Eq. (1)].

TABLE I. Parameters of undoped (Ref. 10), Ni- and Cr-doped $\beta$-iron disilicide single crystals. The meaning of the symbols is explained in the text.

| Sample | $\chi_0$[a] $10^{-6}$ (emu/gOe) | A[a] $10^{-5}$ (emu K/gOe) | B[a] $10^{-5}$ (emu $K^{1/4}$/gOe) | $\varepsilon$[a] (meV) | $-\theta$[a] (K) | $T_{0M}$ (K) | $T_{VM}$ (K) | $T_{0SE}$ (K) | $T_{VSE}$ (K) | $\Delta$ (meV) |
|---|---|---|---|---|---|---|---|---|---|---|
| Undoped[b] | 0.4 | 2.7 | −0.14 | 95 | 100 | | | | | |
| | (0.2) | (0.3) | (0.01) | (10) | (10) | | | | | |
| Ni-doped | 3.0 | 25 | −16 | 158 | 162 | 468 | 130 | 12 | 11 | 0.5 |
| | (0.3) | (1) | (2) | (10) | (10) | (22) | (10) | (1) | (1) | (0.05) |
| Cr-doped | | | | | | 470 | 38 | 39 | 12 | 0.9 |
| | | | | | | (22) | (3) | (2) | (1) | (0.1) |

[a]Parameters were estimated from nonlinear fitting (using Origin 7). The bracket values indicate the absolute errors.
[b]Reference 10.

$\chi_p$ is the temperature-dependent susceptibility due to paramagnetic impurities, $\chi_c$ is the magnetic susceptibility due to free carriers, which is temperature dependent. It is assumed that $\chi_c$ and $\chi_0$ are largely independent of the external field $H$, i.e., we remain in the linear-response regime for these two contributions. $\chi_p(T)$ is determined according to a Curie-Weiss law

$$\chi_p = A/(T-\theta), \tag{2}$$

where

$$A = \frac{N_p \mu_B^2 p_{\text{eff}}^2}{3\rho k}, \tag{3}$$

$$p_{\text{eff}}^2 = g^2 S(S+1),$$

$\theta$ is the paramagnetic Curie temperature, $N_p$ is the concentration of the paramagnetic centers, $\mu_B$ is the Bohr magneton, $p_{\text{eff}}$ is the effective number of Bohr magnetons, $g$ is the Landé factor, $S$ is the spin of the paramagnetic center, and $\rho$ is the density of the material (for $\beta$-$FeSi_2$ $\rho = 4.93$ g/cm$^3$, Ref. 10).

The expression for the magnetic susceptibility $\chi_c$ of free carriers, if only one type of carriers is present and the Boltzmann statistics can be applied, is given by[10]

$$\chi_c = \frac{n\mu_B^2}{\rho k t}\left[\frac{g^2}{4} - \frac{1}{3}\left(\frac{m}{m^*}\right)^2\right], \tag{4}$$

where $n$ is the electron (hole) concentration and $m^*$ is the density-of-state-electron (hole) effective mass.

In the samples studied the electron gas is nondegenerate. Estimation of the reduced Fermi level has been done, assuming that $m_n^*/m = 0.6$.[10]

The concentration of free electrons is given by[25]

$$n = \left[\frac{N_\nu}{\gamma} N\right]^{1/2} \exp\left[-\frac{\varepsilon}{2kT}\right], \tag{5}$$

where

$$N_\nu = 2(2\pi m^* kT/h^2)^{3/2} = N_\nu' T^{3/2},$$

$N_\nu$ is the density of states in the conduction (valence) band, $N$ and $\varepsilon$ is the concentration and the activation energy of donor (acceptor) levels, respectively, $\gamma$ is the degeneracy factor ($\gamma = 2$). Taking into account Eqs. (4) and (5), $\chi_c(T)$ can be written as

$$\chi_c = BT^{-1/4} \exp(-\varepsilon/2kT), \tag{6}$$

where

$$B = \frac{\mu_B^2}{\rho k}\left(\frac{N_\nu'}{\gamma} N\right)^{1/2}\left[\frac{g^2}{4} - \frac{1}{3}\left(\frac{m}{m^*}\right)^2\right]. \tag{7}$$

At low temperatures, where it is possible to neglect the $\chi_c(T)$ term on the right-hand side of Eq. (1), this expression reduces to

$$\chi(T) = \chi_o + \chi_p(T). \tag{1a}$$

The experimental curve $\chi(T)$ was satisfactorily fitted, using Eqs. (1), (2), and (6) and $\chi_0$, $A$, $\theta$, $B$, and $\varepsilon$ as adjustable parameters (Fig. 2). The values of $\chi_0$, A, and $\theta$ were preliminarily estimated by fitting the low-temperature part of the curves $\chi(T)$ on the base of Eqs. (1a) and (2). The obtained set of parameters as well as parameters of the undoped $n$-typed $\beta$-iron disilicide single crystal[10] are presented in Table I.

In undoped and Ni-doped samples the values of $\chi_0$ are different (Table I). This can probably be caused by a difference in the concentration and types of lattice defects and/or neutral impurities. However, the measurements performed do not permit to identify lattice defects and neutral impurities or to separate their contribution from the lattice contribution.

The dependence $1/\chi_p$ vs $T$ (where $\chi_p$ is equal to $\chi - \chi_0 - \chi_c$) in accordance with Eq. (2) is a straight line indicating Curie-Weiss behavior (Fig. 3). The values of $\theta$ and $A$ deter-

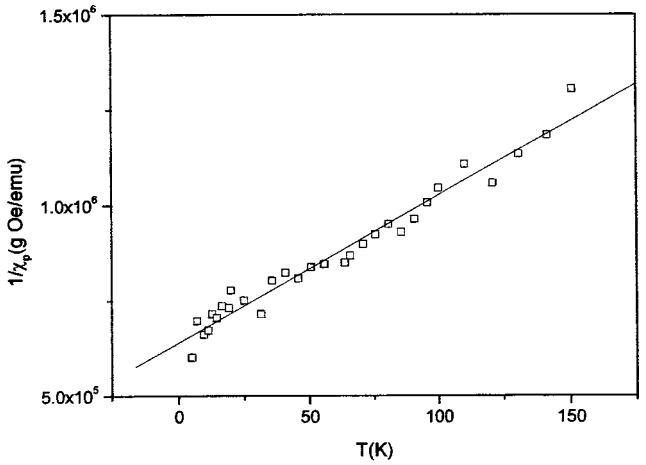


FIG. 3. Dependence of $1/\chi_p$ ($\chi_p$ is the temperature dependent susceptibility due to paramagnetic impurities) vs temperature for the Ni-doped samples.

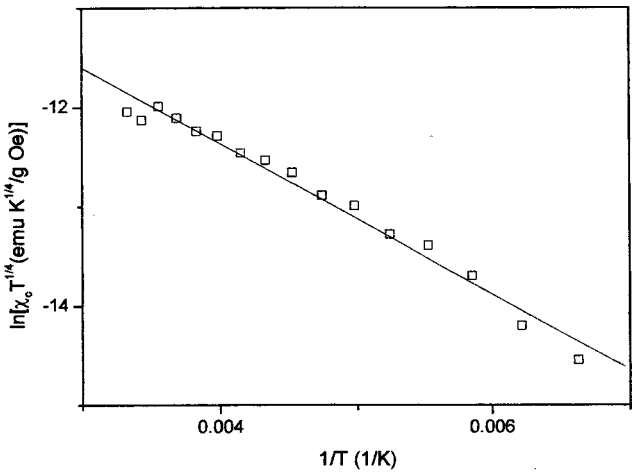


FIG. 4. Dependence of $\chi_c T^{1/4}$ ($\chi_c$ is the magnetic susceptibility due to free carriers) vs $1/T$ for the Ni-doped samples.

mined from their intersection (along $T$ axes) and slope, respectively, in the low-temperature range of the magnetic susceptibility data are in agreement with the values estimated from the fitting of the experimental curve of $\chi(T)$ in the whole temperature region studied. The Curie-Weiss temperature is negative both in undoped and in Ni-doped samples (Table I) and indicates antiferromagnetic interactions in these $\beta$-iron disilicide crystals.

Concentration of Cr and Ni in our samples are unknown and it is difficult to make reliable conclusions about the valence states of Cr and Ni impurities from our magnetic measurements. Some conclusions could be done on the basis of the EPR data, however, available literature data are not in agreement. According to Ref. 16 centers with $S=1/2$ are observed and their origins are $Ni^+$ and $Cr^-$ ions substituting for Fe on one of its two inequivalent lattice sites; Aksenov *et al.*[18] observed the doublet signal believed to arise from spin triplet ($S=1$) states of, presumably, substitutional $Ni^{2+}$ transition ions.

The plot of $\ln(\chi_c T^{1/4})$ vs $1/T$ (where $\chi_c$ is equal to $\chi - \chi_0 - \chi_p$) yields a straight line in the high-temperature region (Fig. 4). Its slope was used to estimate the value of the donor levels activation energy in Ni-doped samples according to Eq. (6). The value obtained from analysis of the high-temperature range of the magnetic susceptibility data and the value estimated as an adjustable parameter from the fit to the susceptibility measurements of $\chi(T)$ in the whole temperature region studied are in agreement, equal to about 158 meV and close to those estimated from our resistivity data on Ni-doped (181 meV) samples. The determined value of $B$ (Table I) is negative in Ni-doped $n$-type crystals. The negative sign of $B$ observed also in undoped $n$-type $\beta$-$FeSi_2$ crystal[10] indicates, in accordance with Eq. (7), that the absolute value of the diamagnetic term in $n$-type studied crystals is somewhat higher than the paramagnetic term.

Above, we have analyzed results for the magnetic susceptibility data taken at 1 kOe. It should be mentioned that a careful study of the Cr and Ni-doped crystals showed that in a weaker external magnetic field the field-cooled (FC) and zero-field-cooled (ZFC) magnetization are different. The difference is slight but can be reliably determined below

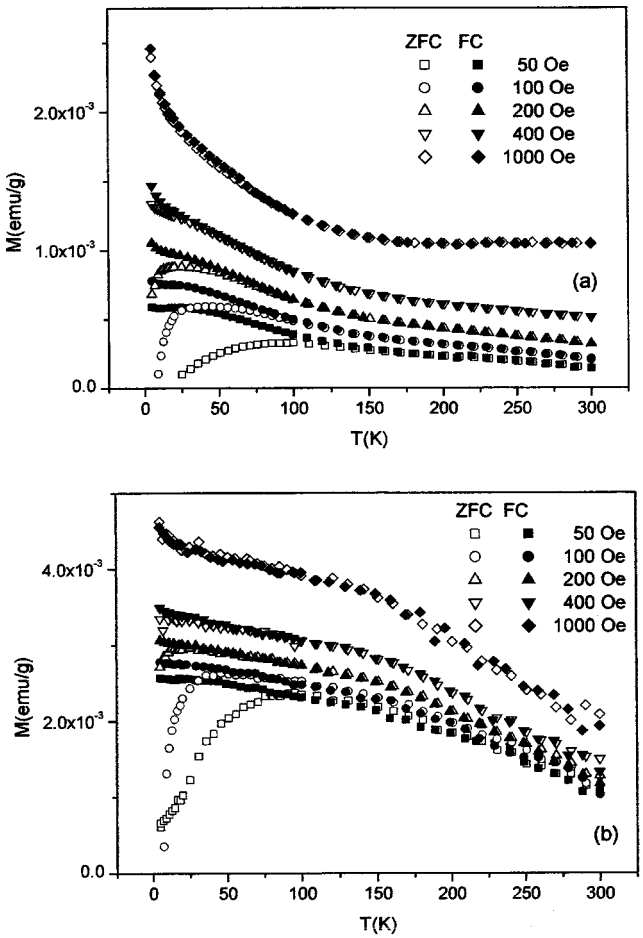


FIG. 5. Zero-field-cooled (ZFC, open symbol) and field-cooled (FC, closed symbol) specific magnetization for Cr-doped (a) and Ni-doped samples (b) in the field of 50, 100, 200, 400 and 1000 Oe.

100–150 K [Figs. 5(a) and 5(b)]. It is well pronounced in both samples for 50, 100, and 200 Oe and it can still be resolved in Cr-doped samples for 400 Oe. No difference is observed, when a stronger field (1000 Oe) is applied [Figs. 5(a) and 5(b)]. This is consistent with a small remanent magnetization component observed in the $M(H,T)$ data. These peculiarities of the magnetic properties in weak fields remind us of those observed in spin glasses or cluster glasses. Our data can be qualitatively understood by either freezing of magnetic clusters, or by a magnetic coupling between the paramagnetic centers which brings about cooperative magnetic freezing as in a dilute spin-glass system.[26] The magnetic signal of our samples is rather low. Therefore, a detailed investigation of thermomagnetic behavior and possible glassy dynamics could not yet be achieved.

### B. Electrical properties: Hopping mechanisms

The temperature dependence of the resistivity $\rho$ of the investigated crystals is shown in Fig. 6. The conductivity has an activated character, including two intervals with different slopes of the function of $\rho(1/T)$. The first interval at high temperatures is connected with the band conduction [activation of carriers from donor (acceptor) levels to the conduction (valence) band]. The activation energy of the Cr acceptor (138 meV) and the Ni donor (181 meV) was determined

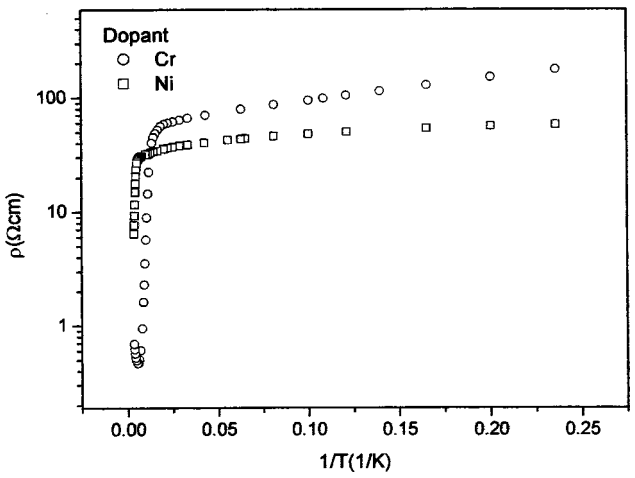


FIG. 6. Temperature dependence of the resistivity in the Cr- and Ni-doped samples.

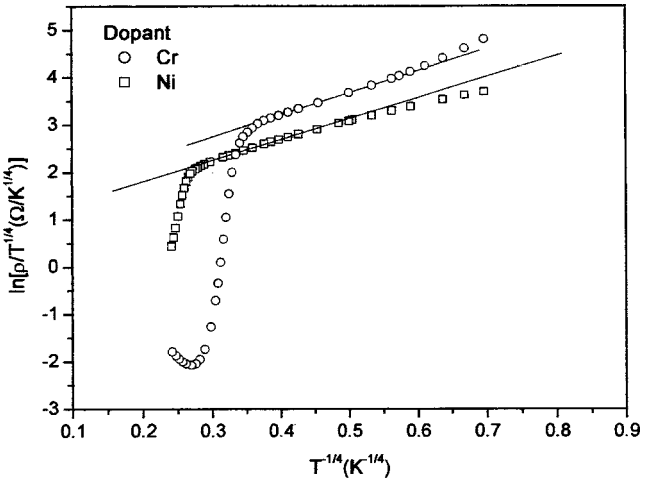


FIG. 7. The dependence of $\ln(\rho/T^{1/4})$ on $T^{1/4}$ in Cr-doped and Ni-doped samples.

assuming that $\rho \propto \exp(\varepsilon/(2k_BT))$ in accordance with Eq. (5). The values are about two times higher than those estimated from the resistivity data on Cr-doped [85 meV (Refs. 20 and 21)] and Ni-doped [95 meV (Ref. 20)] samples assuming $\rho \propto \exp(\varepsilon/(2k_BT))$. The activation energy of the Ni donor (181 meV) is in agreement with that determined from our magnetic measurements data (Table I). The slope in the low-temperature interval is determined by the hopping conductivity, or transitions between the impurity centers or localized states inside the impurity band. The low-temperature slope is not constant but varies with temperature suggesting variable-range hopping (VRH) conduction. Two different types of VRH should be distinguished. Mott (M) type of VRH takes place when the electron density of states (DOS) ($\mu$), at the Fermi level $\mu$ is constant,[27] and Shklovskii-Efros (SE) type of VRH is found when the DOS has a parabolic quasigap due to the long-range Coulomb correlations of the localized electrons in the energy range between $\mu$-$\Delta$ and $\mu+\Delta$.[28] The resistivity in the range of VRH conduction can be expressed as

$$\rho(T) = \rho_{0M} \exp[(T_{0M}/T)^p], \quad \rho(T) = \rho_{0SE} \exp[(T_{0SE}/T)^p], \tag{8}$$

where $p=1/4$ (M-VRH) or $1/2$ (SE-VRH), $\rho_{0M}=A_M T^{1/4}$ and $\rho_{0SE}=A_{SE}T^{1/2}$ are the prefactors ($A_M$ and $A_{SE}$ are independent of $T$), and $T_{0M}$ and $T_{0SE}$ are the characteristic M-VRH and SE-VRH regime hopping temperatures, respectively. $T_{0M}$ and $T_{0SE}$ can be expressed as[28]

$$T_{0M} = \frac{\beta_M}{k_B g_n(\mu)\alpha^3}, \quad T_{0SE} = \frac{\beta_{SE}e^2}{\kappa k_B \alpha} \tag{9}$$

where $\beta_M=21$, $\beta_{SE}=2.8$ are numerical constants, $\kappa$ is the dielectric permeability, $g(\mu)$ is the density of the localized states, and $\alpha$ is the localization radius of charge carriers.

The value of the width of the quasigap $\Delta$ is given by[28]

$$\Delta = \frac{k_B}{2}\sqrt{T_{0SE}T_{VSE}} \tag{10}$$

where $T_{VSE}$ is the temperature for the transition to VRH conduction involving states of the Coulomb gap (SE regime), or for opening of the Coulomb gap.

The regime of the VRH conduction can be determined using two different methods. The first method for conduction mechanism analysis uses plots of the temperature dependence of the resistivity in different coordinates according to Eq. (8). As can be seen from Figs. 7 and 8 our Cr- and Ni-doped samples display both M- and SE-VRH in the low and lowest temperature intervals, respectively. Another method is to determine the hopping regime based on the analysis of the local activation energy,[28] $E_a(T)=d\ln\rho(T)/d(k_BT)^{-1}$, which can be presented using Eq. (8) in the form[29]

$$\ln[E_a/(k_BT)+m] = \ln p + p\ln T_0 + p\ln(1/T), \tag{11}$$

where $m=p$. Namely, by putting $m=1/2$ or $1/4$ in the left-hand side of Eq. (11), from the linear dependence $\ln[E_a/(k_BT)+m]$ vs $\ln(1/T)$ we should obtain $p=1/2$ or $1/4$ provided that one of the two hopping regimes, SE- or M-VRH conductivity, respectively, takes place. As can be seen from Figs. 9(a) and 9(b), the Mott and SE-VRH conductivity is well observed, supporting the conclusion drawn from the plots in Fig. 7. The values of the characteristic temperatures $T_{VM}$, the temperature for the onset of M-VRH,

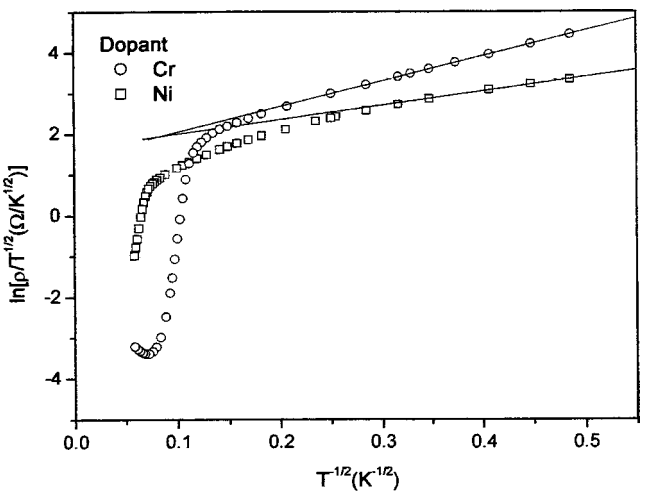


FIG. 8. The dependence of $\ln(\rho/T^{1/2})$ on $T^{1/2}$ in Cr-doped and Ni-doped samples.

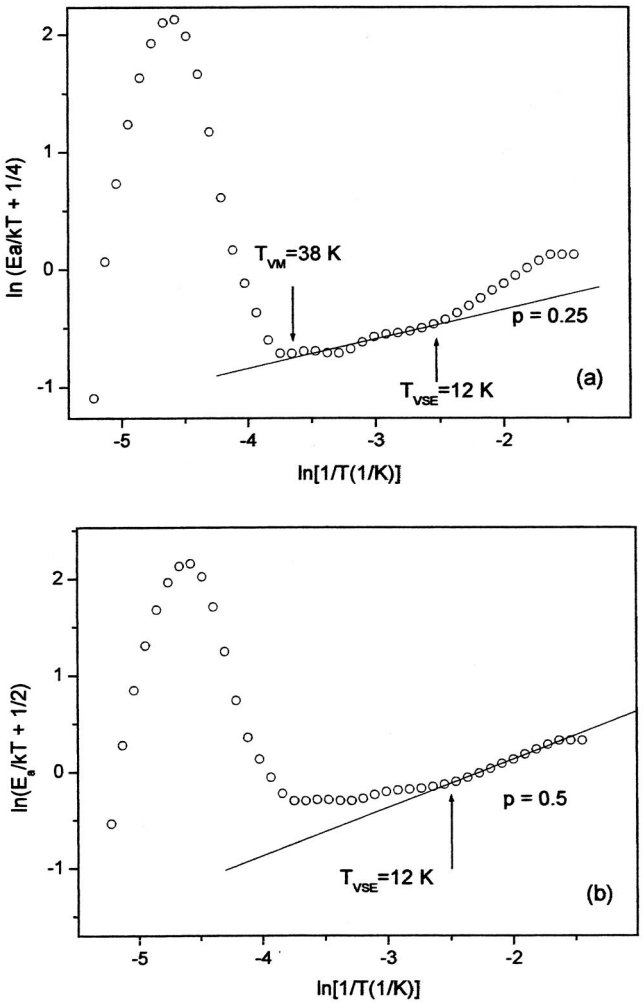


FIG. 9. The dependence of $\ln(E_a/k_BT+1/4)$ vs $\ln(1/T)$ (a) and $\ln(E_a/k_BT+1/2)$ vs $\ln(1/T)$ (b) in Cr-doped samples.

and $T_{\mathrm{VSE}}$, the temperature for the transition to SE-VRH conduction, and those of the characteristic temperatures $T_{0\mathrm{M}}$ and $T_{0\mathrm{SE}}$ determined from the slope of the plots $\ln(\rho/T^p)$ vs $1/T^p$ (see Figs. 7 and 8) agree with the corresponding data obtained from the temperature dependence of the local activation energy. With Eq. (10) we find $\Delta \approx 0.9$ and 0.5 meV in Cr- and Ni-doped samples, respectively. These data are presented in Table I. Our data for the *p*-type Cr-doped sample are in reasonable agreement with those reported for *p*-type Al-doped $\beta$-$FeSi_2$ single crystals.[30] It should be mentioned that hopping conductivity in *n*-type $\beta$ iron-disilicide crystals is reported here. The M-VRH conductivity is observed over a wide temperature range in both *n*- and *p*-type crystals, especially in the Ni-doped *n*-type sample.

The mean hopping length of the M-VRH conductivity is given by[28]

$$R_{h\mathrm{M}} = C_{\mathrm{M}}\alpha\left(\frac{T_{0\mathrm{M}}}{T}\right)^{1/4}, \tag{12}$$

where $C_{\mathrm{M}} \approx 0.357$. In both Cr- and Ni-doped samples the values of $R_{h\mathrm{M}}/\alpha$ are less than 1 in a temperature range where Mott's VRH is observed. This relation between the length scales of the variable-range hopping is indicative of the behavior near a metal-insulator transition.[31]

## IV. SUMMARY

In conclusion, the temperature dependence of the magnetic susceptibility in Ni-doped $\beta$-$FeSi_2$ in the range of 5–300 K can be explained by considering the temperature-dependent parts due to paramagnetic centers and due to the carriers thermally excited in the extrinsic conductivity region. The temperature variation of the paramagnetic terms is in agreement with the Curie-Weiss law. The values of the paramagnetic Curie temperature and the activation energy of the donor and acceptor levels were estimated. A difference between the magnetization in the Cr- and Ni-doped samples cooled in zero magnetic field and in a weak magnetic field is observed and can be explained by assuming that below 150 K collective freezing of magnetic centers occurs in our $\beta$-$FeSi_2$ crystals. The low-temperature resistivity of $\beta$-$FeSi_2$ has also been investigated. Mott- and SE- variable-range hopping conductivity have been observed. The widths of the Coulomb gap in the DOS spectrum have been obtained.

[1] *Semiconducting Silicides*, edited by V. Borisenko (Springer, Berlin, 2000).
[2] H. Lange, Phys. Status Solidi B **201**, 3 (1997).
[3] A. Heinrich, G. Behr, H. Griessmann, S. Teichert, and H. Lange, Mater. Res. Soc. Symp. Proc. **478**, 255 (1997).
[4] D. Leong, M. Harry, K. J. Reeson, and K. P. Homewood, Nature (London) **387**, 686 (1997).
[5] T. Suemasu, Y. Negishi, K. Takakura, and F. Nasegawa, Jpn. J. Appl. Phys., Part 2 **39**, L1013 (2000).
[6] M. Konagai, Proceeding of the 2nd Workshop of "The Path to ultra-high efficient photovoltaics," Joint Research Centre, European Commission, Ispra, 2003, p. 118.
[7] U. Birkholz and A. Frühauf, Phys. Status Solidi **34**, K 81 (1969).
[8] O. Valassiades, C. A. Dimitriadis, and J. H. Werner, J. Appl. Phys. **70**, 890 (1991).
[9] E. Arushanov, Ch. Kloc, H. Hohl, and E. Bucher, J. Appl. Phys. **75**, 5106 (1994).
[10] E. Arushanov, M. Respaud, J. M. Broto, Ch. Kloc, J. Leotin, and E. Bucher, Phys. Rev. B **53**, 5108 (1996).
[11] H. Kakemoto, T. Higuchi, Y. Makita, S. Sakuragi, Y. Kino, T. Tsukamoto, and S. Shin, Physica B **281,282**, 638 (2000).
[12] K. Tagaya, Y. Hayashi, Y. Maeda, K. Umezawa, and K. Miyake, Jpn. J. Appl. Phys., Part 1 **39**, 4751 (2000).
[13] S. Brehme, G. Behr, and A. Heinrich, J. Appl. Phys. **89**, 3798 (2001).
[14] S. Teichert, G. Beddies, Y. Tomm, H.-J. Hinneberg, and H. Lange, Phys. Status Solidi A **152**, K15 (1995).
[15] P. Lengsfeld, S. Brehme, G. Ehlers, H. Lange, N. Stusser, Y. Tomm, and W. Fuhs, Phys. Rev. B **58**, 16154 (1998).
[16] K. Irmscher, W. Gehlhoff, Y. Tomm, H. Lange, and V. Alex, Phys. Rev. B **55**, 4417 (1997).
[17] T. Miki, Y. Matsui, K. Matsubara, and K. Kishimoto, J. Appl. Phys. **75**, 1693 (1994).
[18] I. Aksenov, H. Katsumata, Y. Makita, Y. Kimura, T. Shinzato, and K. Sato, J. Appl. Phys. **80**, 1678 (1996).
[19] G. Behr, J. Werner, G. Weise, A. Heinrich, A. Burkov, and C. Gladun, Phys. Status Solidi A **160**, 549 (1997).
[20] A. Heinrich, H. Griessmann, G. Behr, K. Ivanenko, J. Schumann, and H. Vinzelberg, Thin Solid Films **381**, 287 (2001).
[21] S. Brehme, P. Lengsfeld, P. Stauss, H. Lange, and W. Fuhs, J. Appl. Phys. **84**, 3187 (1998).
[22] E. Arushanov, J. H. Schön, and H. Lange, Thin Solid Films **381**, 282 (2001).
[23] J. Tani and H. Kido, Jpn. J. Appl. Phys., Part 1 **38**, 2717 (1999).
[24] J. Tani and H. Kido, J. Appl. Phys. **84**, 1408 (1998).
[25] J. S. Blakemore, *Semiconductor Statistics* (Pergamon, Oxford, 1962).

[26]E. Arushanov, L. Ivanenko, D. Eckert, G. Behr, U. K. Rößler, K.-H. Müller, S. Schneider, and J. Schumann, J. Mater. Res. **17**, 2960 (2002).
[27]N. Mott and E. A. Davies, *Electron Processes in Non-Crystalline Materials* (Clarendon, Oxford, 1979);N. F. Mott, *Metal-Insulator Transitions* (Taylor and Francis, London, 1990).
[28]B. I. Shklovskii and A. L. Efros, *Electronic Properties of Doped Semiconductors* (Springer, Berlin, 1984).
[29]K. Lisunov, B. Raquet, H. Rakoto, J. M. Broto, E. Arushanov, X. Z. Xu, H. El. Alami, and C. Deville Cavellin, J. Appl. Phys. **94**, 5912 (2003).
[30]K. G. Lisunov, E. Arushanov, Ch. Kloc, U. Malang, and E. Bucher, Phys. Status Solidi B **195**, 227 (1996).
[31]A. Roy, M. Levy, X. M. Guo, M. P. Sarachik, R. Ledesma, and L. L. Isaaks, Phys. Rev. B **39**, 10185 (1989).